Nanoscale

RSC Publishing

PAPER

View Article Online
View Journal | View Issue

Cite this: *Nanoscale*, 2013, **5**, 1583

Enzyme-mimetic effects of gold@platinum nanorods on the antioxidant activity of ascorbic acid†

Yu-Ting Zhou,‡[ab] Weiwei He,‡[ac] Wayne G. Wamer,[a] Xiaona Hu,[d] Xiaochun Wu,[d] Y. Martin Lo*[b] and Jun-Jie Yin*[a]

Received 8th October 2012
Accepted 10th December 2012

DOI: 10.1039/c2nr33072e

www.rsc.org/nanoscale

Au@Pt nanorods were prepared by growing platinum nanodots on gold nanorods. Using electron spin resonance (ESR), we determined that the mechanisms for oxidation of ascorbic acid (AA) by Au@Pt nanorods and ascorbic acid oxidase (AAO) were kinetically similar and yielded similar products. In addition we observed that Au@Pt nanorods were stable with respect to temperature and pH. Using UV-VIS spectroscopy, the apparent kinetics of enzyme-mimetic activity of Au@Pt nanorods were studied and compared with the activity of AAO. With the help of ESR, we found that Au@Pt nanorods did not scavenge hydroxyl radicals but inhibited the antioxidant ability of AA for scavenging hydroxyl radicals produced by photoirradiating solutions containing titanium dioxide and zinc oxide. Moreover, the Au@Pt nanorods reduced the ability of AA to scavenge DPPH radicals and superoxide radicals. These results demonstrate that Au@Pt nanorods can reduce the antioxidant activity of AA. Therefore, it is necessary to consider the effects of using Pt nanoparticles together with other reducing agents or antioxidants such as AA due to the oxidase-like property of Au@Pt nanorods.

Introduction

Because of their substrate specificity and efficient catalytic ability, enzymes have been commercially used in various areas such as sewage treatment, textile finishing, household products preparation, food and beverage processing,[1] and energy conversion.[2] However, since most enzymes are sensitive to environmental conditions and are difficult to prepare in large scale, considerable efforts have been attempted to immobilize enzymes for more convenient preparation and easier separation of the enzyme from the product, thus facilitating reuse of the enzyme.[3] In recent years, finding enzyme alternatives has become possible through advances in nanotechnology.

The unique physical and chemical properties of nanoparticles (NPs) have led to their use in a wide range of applications. Amongst these applications, nanoparticles have been found to be candidates as enzyme mimetics with the advantages of low cost, controlled synthesis, tunable catalytic activities, and high stability even under severe reaction conditions. Currently, peroxidase and oxidase activities have been observed for a number of nanoparticles including ferromagnetic NPs,[4] FeS,[5] CuS,[6] graphene oxide,[7] Co_3O_4,[8] single-walled carbon nanotubes,[9] gold nanoparticles and clusters,[10–13] cerium oxide[14] and platinum nanoparticles.[15,16] These nanoparticles could potentially replace the use of enzymes in biosensors or in biodiagnostic medical devices.

The behavior of nanoparticles as oxidase mimics is of particular interest. In the presence of oxygen, oxidases can oxidatively degrade reducing agents and thus prevent these potent antioxidants from intercepting reactive oxygen species (ROS).[17] Examples of biologically important antioxidants are ascorbic acid, uric acid, and polyphenol, which may be oxidatively degraded by ascorbic acid oxidase, uricase, and polyphenol oxidase, respectively. For example, polyphenol oxidase is the main contributor to fruit or vegetable browning and causes degradation of polyphenols. Therefore, along with the application of nanoparticles as enzyme mimetics, the use of NPs could result in deleterious interactions with antioxidants.

The platinum family of NPs has been explored as multi-enzyme mimetics for potential usage in various fields. For example, Pt NPs have been reported to catalyze the peroxidation of 3,3′,5,5′′-tetramethylbenzidine[18] and *o*-phenylenediamine[16,19,20] in the presence of H_2O_2. In conjunction with glucose oxidase and cholesterol oxidase, Pt NPs have been used as replacements for horseradish peroxidase in biosensors for glucose and cholesterol.[16] Studies have found that bimetallic and biostabilized Pt

[a]*Center for Food Safety and Applied Nutrition, U.S. Food and Drug Administration, College Park, MD 20740, USA. E-mail: junjie.yin@fda.hhs.gov; Tel: +1 240 402 1991*

[b]*Department of Nutrition and Food Science, University of Maryland, College Park, MD 20742, USA. E-mail: ymlo@umd.edu*

[c]*Key Laboratory for Micro-Nano Energy Storage and Conversion Materials of Henan Province, Institute of Surface Micro and Nanomaterials, Xuchang University, Xuchang 461000, China*

[d]*CAS Key Laboratory of Standardization and Measurement for Nanotechnology, National Center for Nanoscience and Technology, Beijing 100190, China*

† Electronic supplementary information (ESI) available: Ascorbic acid oxidase activity of Pt NPs and the effects of Au@Pt nanorods on hydroxyl radicals generated from the Fenton reactions and TiO_2 exposed to UV radiation. See DOI: 10.1039/c2nr33072e

‡ Both authors contributed equally.

NPs can scavenge the superoxide radical (O_2^{-}) like superoxide dismutase and reduce H_2O_2 to oxygen like catalase.[21–23] In addition to their peroxidase-like activity, Pt NPs have been found to resemble uricase in catalyzing oxidation of uric acid.[15]

Several investigators have examined the biochemical properties of Pt NPs. Rehman *et al.* have observed reduced inflammatory responses in macrophages treated with Pt NPs.[24] Kim *et al.* reported that treatment with Pt NPs extended the lifespan of *C. elegans*.[25] Hamasaki *et al.* found that Pt NPs lacked cytotoxicity. These investigators also determined that Pt NPs scavenged intracellular ROS such as superoxide radicals and hydrogen peroxide, and protected cells from toxicity elicited by these ROS.[26] Additionally, Pt NPs have been found to inhibit fatty acid peroxidation and scavenge DPPH radicals, indicating their ability to efficiently intercept free radicals.[27] These studies demonstrated that Pt NPs are excellent antioxidants. While these studies demonstrated that Pt NPs are excellent antioxidants, they did not provide direct evidence that Pt NPs scavenged the most physiologically important radical, hydroxyl radicals. Also, as with many antioxidants, Pt NPs may also exhibit pro-oxidant activity under some conditions. To date, little is known about the interactions between Pt NPs and biologically important antioxidants.

Ascorbic acid (AA), a phytonutrient abundant in fruits and vegetables, is known to protect human body against chronic diseases due to its antioxidant properties and has been widely used in foods, dietary supplements, cosmetic products, *etc.* However, AA is easily degraded through oxidation, especially in the presence of ascorbic acid oxidase (AAO), which exists endogenously in the extracellular matrix of plant cells. AAO mimetics may also reduce the antioxidant activity of AA. Therefore, it is important to identify any AAO-mimetic activity of Pt NPs and understand the interaction between Pt NPs and AA under conditions expected in commercial products.

In the current study, Au@Pt nanorods have been found to act as AAO mimetics in catalyzing oxidation of AA to ascorbyl radicals in the presence of O_2, which can be detected by Electron Spin Resonance (ESR). ESR spectroscopy with spin trapping is the most reliable and direct method for identification and quantification of short-lived free radicals. Radicals such as ascorbyl radicals can be directly detected *via* ESR. However, more reactive radicals, such as hydroxyl radicals and superoxide anions, require the use of spin traps for ESR detection.[17,28,29] In addition, ESR was used to compare the thermal and pH stability of Au@Pt nanorods and AAO. The reaction kinetics of AAO and Au@Pt nanoparticles were determined by UV-VIS spectroscopy. Using the ESR spin trapping technique, we examined the role of Au@Pt nanorods in scavenging hydroxyl radicals, generated through the Fenton reaction and through excitation of metal oxides with UV radiation. Using three radical generation systems, we compared the antioxidant activity of AA alone and its combined effect with Au@Pt nanorods.

Experimental

Materials

Sodium borohydride ($NaBH_4$), gold(III) chloride hydrate ($HAuCl_4 \cdot 3H_2O$), cetyltrimethylammonium bromide (CTAB), potassium tetrachloroplatinate(II) (K_2PtCl_4), and poly-(styrenesulfate) (PSS) were all purchased from Alfa Aesar (Ward Hill, MA) and used as received. The spin traps, 5,5-dimethyl-1pyrroline *N*-oxide (DMPO) and 5-(diethoxyphosphoryl)-5-methyl-1-pyrroline-*N*-oxide (DEPMPO) were purchased from Radical Vision (Marseille, France). The spin trap 5-*tert*-butoxycarbonyl-5-methyl-1-pyrroline-*N*-oxide (BMPO) (Alexis® Biochemicals) was obtained from Enzo Life Science, Inc (Farmingdale, NY). Aeroxide® TiO_2 P25 was a gift from EVONIK Industries AG (Frankfurt, Germany). The spin label 3-carbamoyl-2,5-dihydro-2,2,5,5-tetramethyl-1*H*-pyrrol-1-yloxyl (CTPO), ascorbate oxidase, 1,1-diphenyl-2-picryl-hydrazyl radical (DPPH), L-ascorbic acid (AA), ammonium iron(II) sulfate heptahydrate, ZnO, 30% H_2O_2 aqueous solution, and standard buffer solutions were all purchased from Sigma Aldrich (St. Louis, MO). Platinum nanoparticle dispersion (3 nm, spherical Pt NPs with no coating) was purchased from US Research Nanomaterials, Inc. (Houston, TX). Each buffer stock solution (pH 1.2 HCl–KCl, pH 4.6 HAc–NaAc, pH 7.4 PBS, pH 9.0 borax and pH 11.0 borax) was 0.1 M. Before use, each buffer was treated with Chelex® 100 molecular biology grade resin from Bio-Rad Laboratories (Hercules, CA) to remove trace metal ions. Milli-Q water (18 MΩ cm) was used for preparation of all solutions.

Synthesis of Au@Pt nanorods coated with PSS

The entire preparation procedure has been described in a previous study.[30] Firstly, gold nanorods were prepared *via* seed-mediated growth. CTAB-capped Au seeds were synthesized through chemical reduction of $HAuCl_4$ by $NaBH_4$. After 30 min, growth solution for Au nanorods, consisting of 0.1 M CTAB, 0.024 M $HAuCl_4$, 0.5 M H_2SO_4, 10 mM $AgNO_3$ and 0.1 M AA, was added to Au seeds to initiate the growth of Au nanorods. After 12 h, the Au nanorods were purified by centrifugation (12 000 rpm, 5 min) and the precipitates were collected and resuspended in deionized water for further use. Secondly, the Au nanorod suspension was mixed with a 2 mM K_2PtCl_4 solution. Then, 0.1 M AA was added to the mixture which was shaken vigorously, and then placed in a 30 °C water bath. Formation of Au@Pt nanorods was evidenced by a color change from pink-red to dark grey. Additional 0.1 M CTAB was further added to stop the reaction and prevent aggregation of the nanorods. The suspension was centrifuged (10 000 rpm, 5 min) once more and the precipitate was redispersed in deionized water. Lastly, the Au@Pt nanorod solution was mixed with PSS solution, containing 20 mg ml^{-1} PSS and 60 mM NaCl, and placed at 30 °C for at least 3 h. Subsequently, the reaction mixture was centrifuged (10 000 rpm, 5 min) again to remove excess PSS. The precipitate was redispersed in deionized water for future use. The concentration of Au@Pt nanorods stock solution was 5 nM, which was used to study their enzyme mimetics activity, and the atomic concentration of the Pt nanodots was 1 mM, which was used to study their effect on free radicals. Unless otherwise stated, this nanorod concentration has been used in the current study.

Characterization of Au@Pt nanorods

Scanning electron microscopy (SEM) images were taken on a field emission scanning electron microscope (FESEM, Hitachi

S-4800). High-resolution transmission electron microscopy (HRTEM) images and selected-area electron diffraction patterns were captured at an accelerating voltage of 200 kV from the same microscope.

Kinetic parameters using UV-Vis spectroscopy

UV-vis absorption spectra were obtained using a Varian Cary 300 spectrophotometer. The oxidation of AA catalyzed by AAO or Au@Pt nanorods in buffers at different pHs was performed at 20 °C as follows: AA was mixed with different pH buffers and made up with H_2O to a final concentration of 5 mM or 10 mM. Then, sufficient AAO or Au@Pt nanorods were added to give a final concentration of 0.09 nM or 0.05 nM, respectively. The reaction kinetics for the catalytic oxidation of AA were studied by recording the absorption spectra at 1 min intervals in the scanning kinetics mode. The disappearance of AA was monitored by measurement of its absorbance at the λ_{max} appropriate for each pH. The kinetic parameters were calculated based on the Michaelis–Menten equation $v = V_{max} \times [S]/(K_m + [S])$, where v is the initial velocity, V_{max} is the maximal reaction velocity, [S] is the concentration of substrate and K_m is the Michaelis constant.

ESR measurements

Samples were put in 50 μl glass capillary tubes and placed in the ESR cavity. All ESR measurements were carried out using a Bruker EMX ESR spectrometer (Billerica, MA) at an ambient temperature.

Oxidation of AA catalyzed by Au@Pt nanorods

Ascorbyl radical is an intermediate formed during the oxidation of ascorbic acid by oxygen. ESR can directly detect this radical which has a 10 min half-life.[31] Au@Pt nanorods at different concentrations were added to 5 mM AA in 50 mM PBS buffer (pH 7.4) to start the reaction. The peak-to-peak value of the first line of the ascorbyl radical ESR spectrum was recorded to indicate the amount of ascorbyl radical formed. Spectra were recorded under the following conditions: 20 mW microwave power; 1 G field modulation; 25 G scan width.

Thermal stability of Au@Pt nanorods

In order to compare the catalytic activity of AAO and Au@Pt nanorods with respect to temperature, they were pre-incubated at three temperatures 23, 40, and 70 °C for 3 and 6 h in a water bath. Other steps were the same as described in the previous paragraph.

pH dependent enzyme-like activity of Au@Pt nanorods using ESR oximetry

The catalytic activity of AAO and Au@Pt nanorods at different pHs was evaluated through oxygen consumption monitoring. ESR spin label oximetry was employed to measure oxygen change during the reaction.[32] Solutions containing 0.1 mM of the water-soluble spin label CTPO and 1 mM AA in 50 mM buffers with various pHs were studied. AAO or Au@Pt nanorods were added to initiate the catalytic oxidation of ascorbic acid. The capillary tube was then sealed and positioned in the ESR instrument. ESR spectra were then recorded at 0.5, 1.5, 3, 5, 8, and 10 min at the low field line of CTPO (at 23 °C). Signals were obtained with a 1 G scanning width, 1 mW incident microwave power, and with 100 kHz field modulation.

Scavenging effect of Au@Pt nanorods on hydroxyl radicals

Effects of Au@Pt nanorods on hydroxyl radicals generated by the Fenton reaction. Solutions containing $FeSO_4$, H_2O_2, and the spin trap DEPMPO in PBS buffer were used to study scavenging of hydroxyl radicals generated through the classical Fenton reaction.[33] Hydroxyl radicals (˙OH) were trapped by DEPMPO as the spin adduct DEPMPO/˙OH. To assess whether Au@Pt nanorods scavenged hydroxyl radicals or interacted with the Fenton reagents, the nanorods were first mixed with either iron or hydrogen peroxide for different time periods. Also, ascorbic acid was used to compare the hydroxyl radical scavenging activities of ascorbic acid and Au@Pt nanorods.

In order to investigate the effect of Au@Pt nanorods on the antioxidant property of ascorbic acid, the same Fenton reaction system was employed except that spin trap DMPO was used instead of DEPMPO to detect hydroxyl radicals as the spin adduct DMPO/˙OH. Ascorbic acid, Au@Pt nanorods, or their mixture were premixed at room temperature for 48 h. Then, they were individually introduced into a freshly prepared Fenton reaction system. Generation of hydroxyl radicals was initiated by adding H_2O_2.

Spectra were recorded under the following conditions: 20 mW microwave power; 1 G field modulation; 100 G scan width.

Effects of Au@Pt nanorods on hydroxyl radicals generated by TiO_2 and ZnO/UV. Metal oxides TiO_2 (P25) and ZnO were irradiated at 320 and 340 nm, respectively, to generate hydroxyl radicals, which were trapped by the spin trap DMPO in the form of the spin adduct DMPO/˙OH. Using this method for generation of hydroxyl radicals, we examined quenching of hydroxyl radicals by AA, Au@Pt nanorods, or a combination of AA and Au@Pt nanorods. Spectra were recorded 1 min after the initiation of exposure to UV light under the following conditions: 20 mW microwave power; 1 G field modulation; 100 G scan width.

Effect of Au@Pt nanorods on the antioxidant property of ascorbic acid

Effects of Au@Pt nanorods on the DPPH radical. DPPH radical (DPPH˙) is a stable, nitrogen-centered free radical. The attenuation of its ESR signal is one of the methods widely used to demonstrate a chemical's ability to scavenge free radicals. The effect of ascorbic acid, Au@Pt nanorods, and their combination on the ESR spectrum of DPPH˙ was examined. Ascorbic acid, Au@Pt nanorods, or their mixture were stored at room temperature for 24 h. Afterwards, they were individually added to a control sample containing DPPH˙, ethanol, and 10 mM PBS buffer. The reaction was initiated by adding DPPH˙. Spectra were obtained at 2.5 min using 15 mW incident microwave power and 100 kHz field modulation of 2 G.

Effects of Au@Pt nanorods on the superoxide radical generated by xanthine/xanthine oxidase. Superoxide radicals ($^{\cdot}$OOH) were produced using the xanthine/XOD system and trapped as the spin adduct BMPO/OOH. The method of superoxide radical detection using spin trap BMPO was essentially the same as described by Yin *et al.*[33] Ascorbic acid, Au@Pt nanorods, or their mixture were stored at room temperature for 48 h. Then, they were individually introduced into a freshly prepared xanthine–XOD mixture where generation of superoxide radical was initiated by addition of XOD. The ESR spectra were recorded at 1.5 min using 20 mW microwave power, 1 G field modulation, and 100 G scan width.

Results and discussion

Synthesis and characterization of Au@Pt nanorods coated with PSS

The TEM image in Fig. 1 shows the core–shell morphology of the Au@Pt nanorods. The Au nanorods, ~10 nm in diameter and ~60 nm in length, served as a template and Pt nanodots, ~3 nm in diameter, were grown on them. It has been reported that Pt nanoparticles, especially smaller than 5 nm, exhibit great catalytic activity.[30] In the current study, Pt nanodots were distributed homogeneously on the surface of Au nanorods (Fig. 1 right), as expected because Pt grows in a Stranski–Krastanov mode.[16] Such nanorods are expected to exhibit greatly enhanced catalytic activity due to the large surface area associated with the small diameter of the nanodots.[30] Also, the Pt/Au interface can result in superior catalytic activity toward redox reactions. Here, the Au@Pt nanorods were coated with PSS to prevent aggregation.

Ability of Au@Pt nanorods to catalyze oxidation of ascorbic acid

Ascorbic acid, an active reducing agent, is oxidized by oxygen slowly. However, oxidation is accelerated by addition of ascorbic acid oxidase (AAO), where the intermediate ascorbyl radical ($AA^{\cdot}$) is an indicator of the oxidation (Scheme 1). The ESR spectrum of $AA^{\cdot}$ is shown in the inset of Fig. 2. We observed a hyperfine splitting constant $\alpha_{H4} = 0.177$ and $g = 2.0052$ that are consistent with previous studies.[34,35] Oxidation of ascorbic acid to $AA^{\cdot}$ was dependent on the concentration of Au@Pt nanorods as shown in Fig. 2. At concentrations of Au@Pt nanorods below 0.5 nM, an increase in the concentration of Au@Pt nanorods resulted in an increase in levels of ascorbyl radicals. At higher concentrations of Au@Pt nanorods, no increase in ascorbyl radical levels was observed with increasing nanorod concentration. The saturation of ascorbyl radical formation likely resulted from the depletion of one or both substrates (oxygen and ascorbic acid). The ascorbyl radical was not formed when the reaction solution was deoxygenated with nitrogen in the presence of either AAO or Au@Pt nanorods (data not shown), indicating that Au@Pt nanorods are a catalyst rather than an oxidant. A similar experiment was conducted except that Au@Pt nanorods were replaced with Pt nanoparticles. We observed that the $AA^{\cdot}$ production was also dependent on the concentration of Pt NPs (Fig. S1A†). Furthermore, we found out that with regard to $AA^{\cdot}$ production, Au@Pt nanorods were much more efficient than Pt NPs. This may be due to a number of factors including resistance toward aggregation for Au@Pt nanorods and the promotional effect on catalytic activity of Au nanorods.[36]

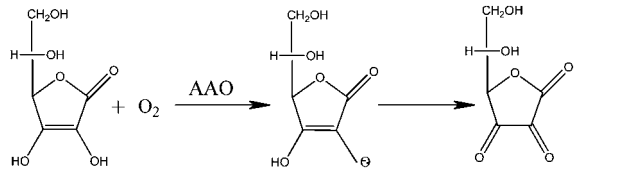

Scheme 1 Enzymatic oxidation of ascorbic acid in the presence of oxygen.

Thermal stability of Au@Pt nanorods as AAO mimetics

Enzymes are sensitive to temperature changes and may be denatured upon heating. By contrast, Au@Pt nanorods are expected to be relatively insensitive to changes in temperature. We compared the thermal stability of Au@Pt nanorods and AAO as shown in Fig. 3. Here, the ascorbyl radical was used as an

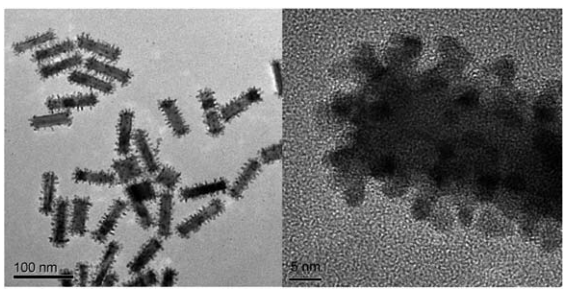

Fig. 1 Morphology of the core–shell structure of Au@Pt nanorods. TEM image (left) and high resolution TEM image (right).

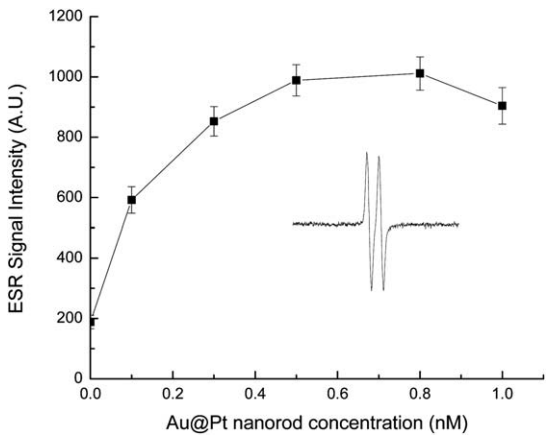

Fig. 2 Ascorbyl radical production is dependent on the concentration of Au@Pt nanorods. Samples contained 5 mM AA and Au@Pt nanorods at variable concentrations in 50 mM PBS (pH 7.4). The inset shows the ESR spectrum of the ascorbyl radical. The ESR signal intensity was measured as the peak-to-peak value of the first line of the spectrum. ESR spectra were collected at 1 min after sample mixing.

indicator of oxidation, where the intensity of the ESR spectrum of ascorbyl radical represented the amount of oxidation product. Both AAO and Au@Pt nanorods were preincubated at 23, 40, and 70 °C in a water bath for 0, 3, or 6 hours prior to examining their effects on oxidation of a freshly made AA solution. A time dependent decrease in the activity of the enzyme, AAO, was observed at all temperatures. Higher temperatures resulted in more rapid decreases in the activity of AAO (Fig. 3, left). However, Au@Pt nanorods were much more stable than AAO during preincubation for up to 6 h. The activity of Au@Pt nanorods in catalyzing the oxidation of AA remained above 95% (Fig. 3, right), which indicates the superior thermal stability of Au@Pt nanorods.

pH dependent activity of AAO and Au@Pt nanorods as AAO mimetics

The stability of ascorbyl radicals varies with reaction conditions such as pH. Therefore, oxygen consumption was used to examine the effects of pH on the oxidation of AA catalyzed by AAO or Au@Pt nanorods. Oxygen consumption was measured by ESR oximetry. The ESR spin label CTPO, in a closed chamber, was used to monitor oxygen concentrations during the oxidation of AA. The ESR spectrum of the spin label CTPO exhibits three lines because of the hyperfine interaction of the unpaired electron with the nitrogen nucleus. Each line is further split into another group of lines because of proton super hyperfine interaction.

The resolution of the super hyperfine structure of the low-field line of the ESR spectrum of CTPO depends on the oxygen concentration of the sample solution. Fig. 4 shows the evolution of the CTPO spectrum during oxidation of AA catalyzed by Au@Pt nanorods. A time dependent increase in super hyperfine splitting was observed. This indicates the disappearance of oxygen in solution during oxidation of AA catalyzed by Au@Pt nanorods. Quantitative estimates of oxygen consumption were obtained from the calibration chart relating the K parameter to oxygen concentration, where K was calculated based on the super hyperfine splitting shape of the ESR spectrum.[32] Herein, the consumption rate of oxygen was used to indicate the apparent activity of both AAO and Au@Pt nanorods. The Pt NPs also catalyzed the oxidization of AA in the presence of oxygen (Fig. S1B†). It is well established that oxidative degradation of AA is enhanced at increased pH, however the rate of the uncatalyzed degradation is relatively low. Thus, the reaction rate is mainly dependent on the catalytic activity. The usual pH-dependence for enzyme activity is a bell shaped curve. The optimum pH range of AAO is reported to be 4–8, which is consistent with our finding that AAO was less active under extreme acidic or alkaline condition (Fig. 5). By contrast, the apparent activity of Au@Pt nanorods increased rapidly with increasing pH (Fig. 5). This may be attributed to the coating material, PSS, which is negatively charged and may make the nanorods more homogenously distributed under alkaline condition. These results demonstrate that Au@Pt nanorods are much more stable catalysts than AAO over a wide range of pHs.

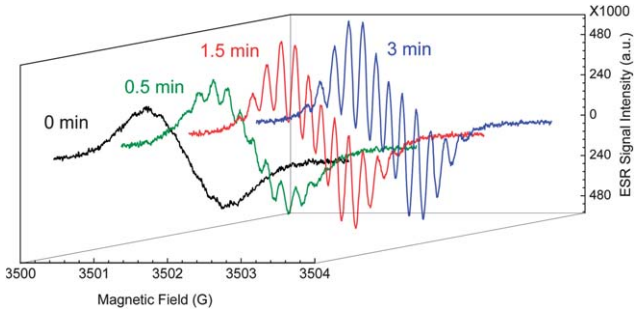

Fig. 4 Evolution of the ESR spectrum of the spin label CTPO during the oxidation of AA catalyzed by Au@Pt nanorods. Sample solutions contained 0.1 mM CTPO, 5 mM AA, and 50 mM PBS (pH 7.4), in the absence (control) and in the presence of 0.5 nM Au@Pt nanorods. ESR spectra were obtained at 0.5, 1.5, and 3 min after addition of Au@Pt nanorods.

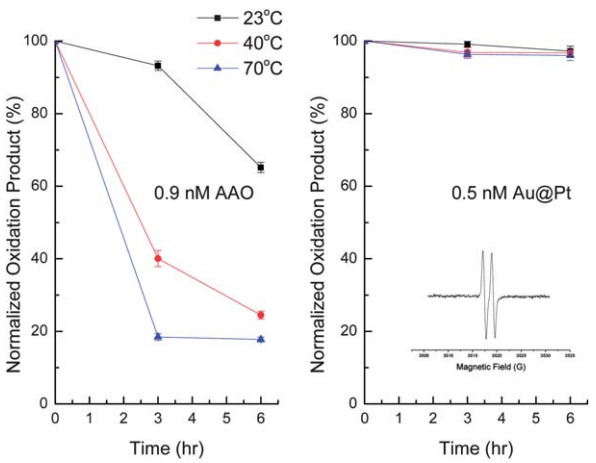

Fig. 3 Thermal stability of AAO and Au@Pt nanorods. 0.9 nM AAO and 0.5 nM Au@Pt nanorods were preincubated at 23, 40, or 70 °C for 0, 3, and 6 h prior to oxidation reaction of 5 mM AA in 50 mM PBS (pH 7.4). The inset represents the ESR spectrum of the ascorbyl radical. The signal intensity was measured as the peak-to-peak value of the first line of the spectrum. ESR spectra were collected at 1 min after sample mixing.

The catalytic mechanism for the nanorods may be attributed to the surface-mediated electron transfer between two substrates. The Michaelis constant (K_m) and catalytic constant (K_{cat}) are key characteristics to describe properties of enzymes. A low K_m represents high affinity between a substrate and an enzyme, while a high K_{cat} indicates a high catalytic ability of the enzyme. Using AA as the substrate, values for K_m and K_{cat} were determined for both AAO and Au@Pt nanorods over the pH range described in Table 1. Under neutral conditions, the K_m of Au@Pt nanorods was much higher than that of AAO, which suggests that binding of AA to AAO is more specific than binding to Au@Pt nanorods. In contrast, the K_{cat} of Au@Pt was many times higher than that of AAO. This demonstrates that Au@Pt nanorods catalyzed the enzymatic reaction more rapidly than AAO, although they had less affinity for the substrate. Our results are consistent with previous findings that Pt nanoparticles behaved similarly as peroxidase,[16,18,19,29] catalase,[23] and uric acid oxidase;[15] Au@Pt nanorods are therefore potentially broad enzyme mimetics.

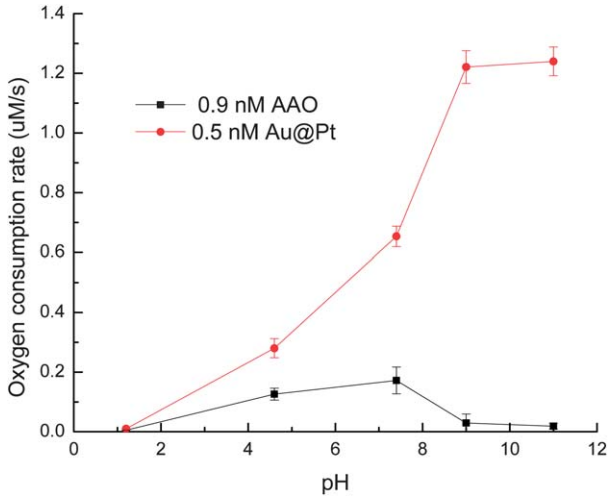

Fig. 5 Ability of AAO and Au@Pt nanorods in catalyzing AA oxidation determined by initial O_2 consumption over a wide pH range. Sample solutions included 0.1 mM CTPO, 5 mM AA, and 50 mM buffers at different pHs.

Table 1 Kinetic parameters for 0.09 nM AAO and 0.05 nM Au@Pt nanorods as AAO mimetics. K_m is the Michaelis constant, V_{max} is the maximum reaction rate and K_{cat} is the catalytic constant. *Reaction conditions*: 50 mM buffers at 23 °C. The reaction is monitored through recording the spectrum peak (220–270 nm) of ascorbic acid in UV-VIS spectrophotometer

	K_m, nM		V_{max}, nM s^{-1}		K_{cat}, s^{-1}	
pH	AAO	Au@Pt	AAO	Au@Pt	AAO	Au@Pt
1.2	219	18.4	0.003	0.764	0.028	15.3
4.6	16.5	16.5	0.17	6.57	1.89	131
7.4	3.1	24.5	0.409	2.09	4.54	41.7
9	4.0	29.1	0.484	2.27	5.38	45.5
11	11.9	27.9	0.465	7.12	5.16	142

Inhibitive effect of Au@Pt nanorods on generation of hydroxyl radicals

The hydroxyl radical possesses the highest one-electron reduction potential of all the physiologically relevant ROS and is extremely reactive with almost every type of biomolecule.[37,38] The Fenton reaction, a widely accepted method for generating hydroxyl radicals, was used to examine the interaction between Au@Pt nanorods and hydroxyl radicals (Fig. S2†). ESR spin trapping using the spin trap DEPMPO was employed to detect the short-lived hydroxyl radical in the form of spin adduct DEPMPO/˙OH, which has eight lines with intensity ratios of 1 : 2 : 2 : 1 : 1 : 2 : 2 : 1 and hyperfine splitting parameters of a_P = 47.3 G, a_H = 13.2 G, and a_N = 14.0 G.[39] A significant reduction of the ESR signal for DEPMPO/OH was observed following addition of AA, a well-known scavenger for ROS. Addition of Au@Pt nanorods also reduced the signal intensity suggesting that Au@Pt nanorods behave as antioxidants by quenching hydroxyl radicals. However, an alternative mechanism is inhibition of hydroxyl radical formation through interactions of Au@Pt with H_2O_2 or Fe^{2+}. To distinguish these mechanisms, Au@Pt was mixed with either H_2O_2 or Fe^{2+} for selected times prior to initiating the Fenton reaction. As shown in Fig. S2A and B(d–f),† lower levels of hydroxyl radicals were produced following longer premixing times, indicating that the Au@Pt nanorods reduced hydrogen peroxide and interacted with Fe^{2+}. These results indicate that Au@Pt nanorods act as catalase mimetics, consistent with previous studies,[21,23] and may facilitate the oxidation or other reactions of Fe^{2+} rather than directly scavenging hydroxyl radicals.

Both TiO_2 (P25) and ZnO generate hydroxyl radicals when exposed to UV radiation at 320 and 340 nm, respectively. In irradiated samples containing DMPO and one of the metal oxides, we observed a four-line spectrum with relative intensities of 1 : 2 : 2 : 1, and hyperfine splitting parameters of $a_N = a_H$ = 14.9 G. This ESR spectrum is characteristic for the spin adduct between DMPO and hydroxyl radical (DMPO/OH).[40] In Fig. 6, a substantial level of hydroxyl radicals was produced following irradiation of ZnO or TiO_2. The addition of AA significantly reduced the ESR signal observed for the DMPO/OH adduct. A previous study stated that Pt nanoparticles were able to scavenge ˙OH generated during UV irradiation of H_2O_2.[26] However, we observed no significant reduction in the ESR signal characteristic of the DMPO/˙OH adduct when Au@Pt nanorods were added and observed for hydroxyl radicals (Fig. 6 and S3†). These results indicate that Au@Pt nanorods do not directly scavenge ˙OH. Therefore, reexamination of the aforementioned scavenging effect of Pt NPs towards hydroxyl radicals is warranted to determine the role of their catalase-like ability to degrade H_2O_2,[23] which is also demonstrated in Fig. S2.† It is noteworthy that, when added together with AA, Au@Pt nanorods inhibited the ability of AA to scavenge hydroxyl radicals (Fig. 6). These phenomena were observed in both TiO_2 and ZnO/UV systems. This finding suggests that while Au@Pt nanorods themselves cannot scavenge hydroxyl radicals, they might reduce the antioxidative properties of other antioxidants.

To further investigate the effect of Au@Pt nanorods on the antioxidant activity of ascorbic acid, three systems for generating radicals were employed (Fig. 7).

DPPH radical (DPPH˙) is a stable radical that has been commonly used to evaluate the antioxidant properties of ingredients in foods. Although DPPH˙ is a stable nitrogen-centered radical that has no involvement in physiological processes, attenuation of the ESR signal for DPPH˙ is one of the criteria widely used to demonstrate the ability to scavenge ROS.[41] In Fig. 7A, a characteristic one line spectrum was obtained for the control solution of 0.1 mM DPPH˙ and 10% ethanol in PBS buffer. We observed that the ESR signal for the DPPH radical nearly disappeared when the well-recognized antioxidant, ascorbic acid, was added (Fig. 7A, spectrum 1 compared with spectrum 3). In contrast, Au@Pt nanorods at a concentration of 1.6 μM (Pt nanodots) had little effect in reducing the ESR signal for the DPPH radical. However, after 24 h, the mixture of nanorods (at the same concentration) and AA resulted in a significant increase in the ESR signal compared with the ESR signal observed when only AA was present (Fig. 7A, spectrum 3 compared with spectrum 5). Even when the concentration of Au@Pt nanorods was reduced to an extremely

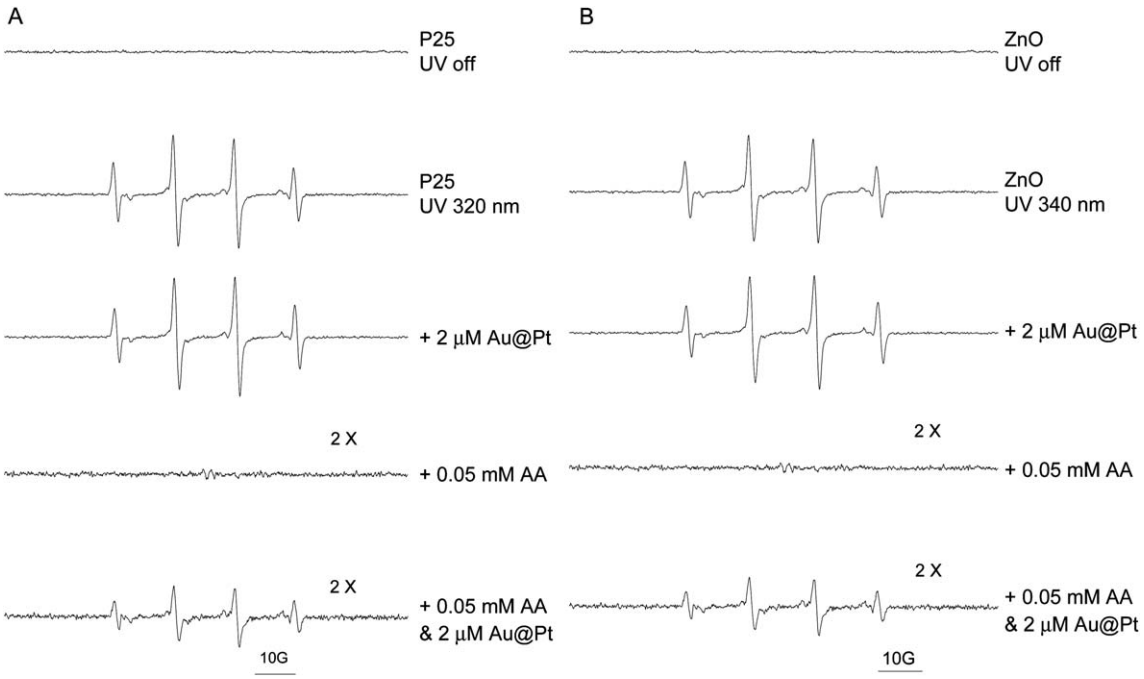

Fig. 6 The effect of Au@Pt nanorods on hydroxyl radical levels and their combined effect with ascorbic acid to scavenge hydroxyl radicals generated during irradiation of metal oxides. (A) Sample solutions containing 0.1 mg ml^{-1} P25 (TiO_2) and 50 mM DMPO were exposed to UV radiation (320 nm). (B) Sample solutions containing 0.1 mg ml^{-1} ZnO and 50 mM DMPO were exposed to UV radiation (340 nm). Samples in A and B contained Au@Pt nanorods, AA, or their combination. ESR spectra were collected at 1 min after UV light was turned on. Pt nanodot concentration was used for Au@Pt nanorods.

low level, 0.8 μM (Pt nanodots), premixing of AA with nanorods still resulted in a significant reduction in AA's antioxidant activity in this system (Fig. 7A, spectrum 4 compared to spectrum 3).

The Fenton reaction is a key contributor to hydroxyl radical generation in biological systems. By means of DMPO, hydroxyl radicals were trapped in the spin adduct DMPO/OH.[40] In biological systems, ascorbic acid is one of the main antioxidants

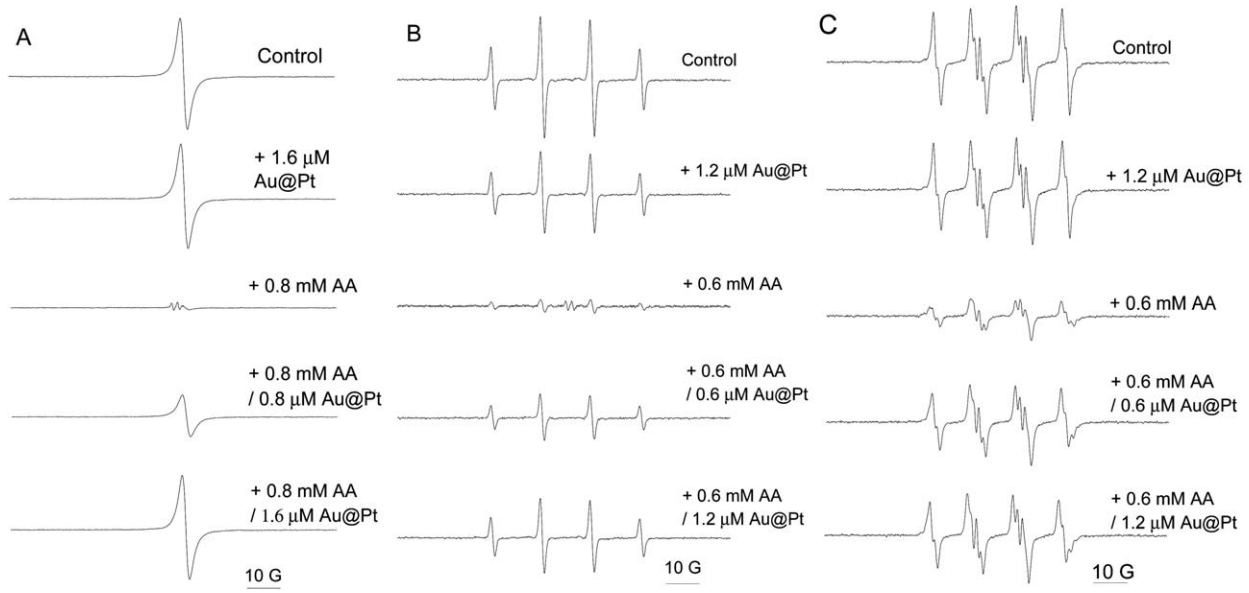

Fig. 7 Effects of Au@Pt nanorods on the antioxidant ability of ascorbic acid. Control sample in (A) contained 0.1 mM $DPPH^{\cdot}$, 10% (v/v) ethanol, and 10 mM PBS buffer (pH 7.4); samples containing AA, Au@Pt nanorods, or a mixture of these were kept at room temperature for 24 h. Control sample in (B) was a Fenton reaction system consisting of 50 mM DMPO, 10 mM PBS buffer (pH 7.4), 0.1 mM Fe^{2+}, and 1 mM H_2O_2; AA, Au@Pt nanorods, or a mixture of these were kept at room temperature for 48 h. Control sample in (C) included 25 mM BMPO, 10 mM PBS buffer (pH 7.4), 1 mM xanthine, and 0.2 U ml^{-1} XOD; AA, Au@Pt nanorods, or a mixture of these were kept at room temperature for 48 h. Pt nanodot concentration was used for Au@Pt nanorods.

that scavenge reactive hydroxyl radicals and thereby prevents oxidative damage in cells. In our model system, a convincing scavenging effect for AA is shown in Fig. 7B, spectrum 3. Au@Pt nanorods also had perceivable inhibitive effect on the hydroxyl radical generation through the Fenton reaction. This may result from its catalytic effect on decomposition of H_2O_2 or oxidation of Fe^{2+} as discussed previously. However, premixing of AA and Au@Pt nanorods for 48 h resulted in a larger ESR signal for the DMPO/OH adduct compared to the ESR signal observed in the presence of AA alone (Fig. 7 B, spectra 3 and 4). Similar results were obtained when the concentration of Au@Pt nanorods was reduced by one half.

In the xanthine/XOD system used for generating superoxide radicals, BMPO was chosen as a spin trap to form the spin adduct BMPO/OOH. The ESR spectrum characteristic for this spin adduct has four lines with relative intensities of 1 : 1 : 1 : 1 and hyperfine splitting parameters of $a_N = 13.4$ and $a_H^\beta = 12.1$.[40] Pt nanoparticles have been reported to be effective superoxide radical scavengers, behaving like SOD.[21] We observed no significant change in the ESR signal for BMPO/OOH when the nanorods were added to the system for generating superoxide radicals (Fig. 7C). It should be noted that we used a much lower concentration of Au@Pt nanorods compared with concentrations of Pt nanoparticles used by investigators reporting quenching of superoxide radicals. As expected, ascorbic acid effectively quenched superoxide radicals resulting in a dramatic reduction in the ESR signal for BMPO/OOH (Fig. 7C, spectrum 3). Premixing AA with Au@Pt nanorods for 48 h resulted in a loss in the ability of AA to quench superoxide radicals as seen by the increase in the ESR signal for BMPO/OOH (Fig. 7C, spectra 3, 4, and 5).

In contrast to previous studies where platinum NPs, at higher concentrations, were capable of quenching DPPH radicals[27] and super oxide radicals,[21] we did not observe the scavenging effect of Au@Pt nanorods under our experimental conditions (Fig. 7). In addition, we find that Au@Pt nanorods do not scavenge hydroxyl radicals, the most reactive biologically relevant free radical (Fig. 6 and S3†). Our results generally suggest that the mechanisms for previously reported radical scavenging by Pt NPs should be reexamined and that indirect mechanisms for radical scavenging should be considered.

Since the human body is not able to synthesize AA, AA must be provided by dietary sources, predominantly fruits and vegetables. AAO is endogenously present in various plants and it is a main factor resulting in enzymatic degradation of AA.[42] The mechanical processing of plants in food production can expose AA to AAO causing degradation of AA, thus reducing antioxidant protection by AA. Platinum nanoparticles have been considered as antioxidants because, under some experimental conditions, they scavenge biologically relevant ROS. Therefore, it is possible that in current or future applications, Pt NPs may be incorporated in complex commercial formulations with multiple components.

In this work, we have found that Au@Pt nanorods and Pt NPs catalyze oxidation of ascorbic acid, acting similar to AAO. As a strong antioxidant, AA scavenges hydroxyl radicals (Fig. 6), DPPH radicals, and superoxide radicals (Fig. 7). Added alone, Au@Pt nanorods, at the concentrations in our study, did not change levels of the above radicals. However, when combined with AA, Au@Pt nanorods significantly reduced the antioxidant property of AA. Our findings suggest that Au@Pt nanorods at the stated levels do not exert antioxidant function in scavenging radicals, but instead can reduce the protective effects of antioxidants such as AA.

Conclusions

In the current study, we have systematically investigated the properties of Au@Pt nanorods as ascorbic acid oxidase mimetics. Commercially available Pt NPs were also found to be AAO mimetics despite their low efficiency. The Au@Pt nanorods were found to be more thermally stable than AAO. In addition, Au@Pt nanorods maintained catalytic activity over a wider pH range than AAO. Results obtained from studying reaction kinetics demonstrated that Au@Pt nanorods were able to rapidly catalyze the oxidation of AA, although AA had a lower affinity to Au@Pt nanorods than to AAO. Similar to the reported peroxidase, catalase, and uricase activities of other Pt nanoparticles, Au@Pt nanorods may be viewed as multienzyme mimetics with broad substrate specificities.

In our study, we examined the radical scavenging ability of Au@Pt nanorods using systems which generated DPPH, hydroxyl or superoxide radicals. No evidence for direct scavenging of these radicals by Au@Pt nanorods was seen under our experimental conditions. Previously reported studies have found that Pt nanoparticles scavenged DPPH and superoxide radicals, but their used experimental conditions were significantly different from ours. Most notably, we have investigated lower concentrations of nanoparticles and have used direct methods for assessing free radical quenching. Au@Pt may exert different effects towards free radicals. Our results indicate that Au@Pt nanorods cannot be simply considered as direct antioxidants, but as enzyme mimetics instead. Consistent with their catalytic activity, trace amounts of Au@Pt nanorods were found to significantly reduce the antioxidant ability of ascorbic acid to scavenge hydroxyl, superoxide, and DPPH radicals. This suggests that as oxidase mimetics, Au@Pt nanorods may have antagonistic effects on antioxidants such as AA. Factors such as experimental conditions, product formulation or product use may dramatically alter the overall effects of Au@Pt nanorods. Therefore, the performance of nanoparticles, such as Au@Pt nanorods, in complex formulations should be evaluated under real use conditions.

Acknowledgements

We thank Dr John Callahan for his valuable discussion and comments. This article is not an official US Food and Drug Administration (FDA) guidance or policy statement. No official support or endorsement by the US FDA is intended or should be inferred. This work was supported by a regulatory science grant under the FY11 FDA Nanotechnology CORES Program.

Notes and references

1 http://biotech.about.com/od/whatisbiotechnology/a/EverydayEnzymes.htm.
2 J. Barber, *Chem. Soc. Rev.*, 2009, **38**, 185–196.
3 W. Tischer and F. Wedekind, in *Topics in Current Chemistry*, ed. W.-D. Fessner, Springer, Heidelberg, 1999, pp. 95–126.
4 L. Gao, J. Zhuang, L. Nie, J. Zhang, Y. Zhang, N. Gu, T. Wang, J. Feng, D. Yang, S. Perrett and X. Yan, *Nat. Nanotechnol.*, 2007, **2**, 577–583.
5 Z. Dai, S. Liu, J. Bao and H. Ju, *Chem.–Eur. J.*, 2009, **15**, 4321–4326.
6 W. W. He, H. Jia, X. Li, Y. Lei, J. Li, H. Zhao, L. Mi, L. Zhang and Z. Zheng, *Nanoscale*, 2012, **4**, 3501–3506.
7 Y. Song, K. Qu, C. Zhao, J. Ren and X. Qu, *Adv. Mater.*, 2010, **22**, 2206–2210.
8 J. Mu, Y. Wang, M. Zhao and L. Zhang, *Chem. Commun.*, 2012, **48**, 2540–2542.
9 Y. Song, X. Wang, C. Zhao, K. Qu, J. Ren and X. Qu, *Chem.–Eur. J.*, 2010, **16**, 3617–3621.
10 J. Jv, B. Li and R. Cao, *Chem. Commun.*, 2010, **46**, 8017–8019.
11 S. Wang, W. Chen, A. Liu, L. Hong, H. Deng and X. Lin, *ChemPhysChem*, 2012, **13**, 1199–1204.
12 X. Wang, Q. Wu, Z. Shan and Q. Huang, *Biosens. Bioelectron.*, 2011, **26**, 3614–3619.
13 N. L. Rosi and C. A. Mirkin, *Chem. Rev.*, 2005, **105**, 1547–1562.
14 A. Asati, S. Santra, C. Kaittanis, S. Nath and J. M. Perez, *Angew. Chem., Int. Ed.*, 2009, **48**, 2308–2312.
15 Y. Dong, Y. Chi, X. Lin, L. Zheng, L. Chen and G. Chen, *Phys. Chem. Chem. Phys.*, 2011, **13**, 6319–6324.
16 J. Liu, X. Hu, S. Hou, T. Wen, W. Liu, X. Zhu, J.-J. Yin and X. Wu, *Sens. Actuators, B*, 2012, **166–167**, 708–714.
17 J.-J. Yin, P. P. Fu, H. Lutterodt, Y. T. Zhou, W. E. Antholine and W. G. Wamer, *J. Agric. Food Chem.*, 2012, **60**, 2554–2561.
18 M. Ma, Yu. Zhang and N. Gu, *Colloids Surf., A*, 2011, **373**, 6–10.
19 W. He, X. Wu, J. Liu, K. Zhang, W. Chu, L. Feng, X. Hu, W. Zhou and S. Xie, *Langmuir*, 2010, **26**, 4443–4448.
20 W. He, X. Wu, J. Liu, X. Hu, K. Zhang, S. Hou, W. Zhou and S. Xie, *Chem. Mater.*, 2010, **22**, 2988–2994.
21 M. Kajita, K. Hikosaka, M. Iitsuka, A. Kanayama, N. Toshima and Y. Miyamoto, *Free Radical Res.*, 2007, **41**, 615–626.
22 L. Zhang, L. Laug, W. Münchgesang, E. Pippel, U. Gösele, M. Brandsch and M. Knez, *Nano Lett.*, 2010, **10**, 219–223.
23 J. Fan, J.-J. Yin, B. Ning, X. Wu, Y. Hu, M. Ferrari, G. J. Anderson, J. Wei, Y. Zhao and G. Nie, *Biomaterials*, 2011, **32**, 1611–1618.
24 M. U. Rehman, Y. Yoshihisa, Y. Miyamoto and T. Shimizu, *Inflammation Res.*, 2012, **61**, 1177–1185.
25 J. Kim, M. Takahashi, T. Shimizu, T. Shirasawa, M. Kajita, A. Kanayama and Y. Miyamoto, *Mech. Ageing Dev.*, 2008, **129**, 322–331.
26 T. Hamasaki, T. Kashiwagi, T. Imada, N. Nakamichi, S. Aramaki, K. Toh, S. Morisawa, H. Shimakoshi, Y. Hisaeda and S. Shirahata, *Langmuir*, 2008, **24**, 7354–7364.
27 A. Watanabe, M. Kajita, J. Kim, A. Kanayama, K. Takahashi, T. Mashino and Y. Miyamoto, *Nanotechnology*, 2009, **20**, 455105–455114.
28 I. Yamazaki and L. Piette, *J. Am. Chem. Soc.*, 1991, **113**, 7588–7593.
29 V. Roubaud, S. Sankarapandi, P. Kuppusamy, P. Tordo and J. Zweier, *Anal. Biochem.*, 1998, **257**, 210–217.
30 W. He, Y. Liu, J. Yuan, J.-J. Yin, X. Wu, X. Hu, K. Zhang, J. Liu, C. Chen, Y. Ji and Y. Guo, *Biomaterials*, 2011, **32**, 1139–1147.
31 G. Rimbach and F. VIrgilli, in *Handbook of Antioxidants*, ed. E.Cadenas and L. Packer, Marcel Dekker Inc, New York, 2002.
32 Y. T. Zhou, J. J. Yin and Y. M. Lo, *Magn. Reson. Chem.*, 2011, **49**, S105–S112.
33 J.-J. Yin, F. Lao, P. P. Fu, W. G. Wamer, Y. Zhao, P. C. Wang, Y. Qiu, B. Sun, G. Xing and J. Dong, *Biomaterials*, 2009, **30**, 611–621.
34 M. K. Sharma and G. R. Buettner, *Free Radical Biol. Med.*, 1993, **14**, 649–653.
35 S. Duan, L. Gu, Y. Wang, R. Zheng, J. Lu, J. Yin, L. Guli and M. Ball, *Am. J. Chin. Med.*, 2009, **37**, 1167–1177.
36 M. Chen, D. Kumar, C.-W. Yi and D. W. Goodman, *Science*, 2005, **310**, 291–293.
37 B. Halliwell and J. M. C. Gutteridge, in *Free Radicals in Biology and Medicine*, Oxford University Press, New York, 2nd edn, 1989, pp. 22–81.
38 G. R. Buettner and B. A. Jurkiewicz, *Radiat. Res.*, 1996, **145**, 532–541.
39 W. He, Y. T. Zhou, W. G. Wamer, M. D. Boudreau and J. J. Yin, *Biomaterials*, 2012, **33**, 7547–7555.
40 H. Zhao, J. Joseph, H. Zhang, H. Karoui and B. Kalyanaraman, *Free Radical Biol. Med.*, 2001, **3**, 599–606.
41 M. C. Foti, C. Daquino and C. Geraci, *J. Org. Chem.*, 2004, **69**, 2309–2314.
42 Y. Shimada and S. Ko, *Chugokugakuen J.*, 2008, **7**, 7–10.